

submitted to ApJL

Delayed Flash from Counter Jet of Gamma Ray Burst

Ryo Yamazaki¹

Department of Physics, Kyoto University, Kyoto 606-8502, Japan

yamazaki@tap.scphys.kyoto-u.ac.jp

and

Kunihito Ioka²

Department of Earth and Space Science, Osaka University, Toyonaka 560-0043, Japan

ioka@vega.ess.sci.osaka-u.ac.jp

and

Takashi Nakamura³

Department of Physics, Kyoto University, Kyoto 606-8502, Japan

takashi@yukawa.kyoto-u.ac.jp

ABSTRACT

If the X-ray flash is the gamma ray burst (GRB) observed with the large viewing angle from the forward jet, we show that the emission from the counter jet should be observed as the *delayed flash* in the UV or optical band several hours to a day after the X-ray flash. If the distance is several tens of Mpc or so, i.e., similar to GRB980425, FUV-MAMA on *HST*/STIS or UVOT on *Swift* can observe the delayed flash, so that the collimated jets of the GRBs may be directly confirmed.

Subject headings: gamma rays: bursts —gamma rays: theory

1. INTRODUCTION

There are several observational implications that the gamma-ray burst (GRB) is caused by the relativistically moving jet (e.g., Frail et al. 2001). However, in order to establish that the GRB is the jet, other observations are indispensable, such as the polarization observation (Ghisellini & Lazzati 1999; Sari 1999) and the microlensing observation (Ioka & Nakamura 2001b). Some theoretical models of the jet emission have been discussed (Totani & Panaitescu 2002; Huang, Dai & Lu 2002; Dado, Dar & De Rújula 2001). If the GRB is the jet, there should be a counter jet, as in the AGN (Begelman, Blandford & Rees 1984) and the microquasar (Mirabel & Rodríguez 1999). Therefore the detection of emissions from the counter jet will give us a direct evidence for the jet model of GRBs.

The confirmation of the counter jet has been by far the important factor in the jet model of astrophysical objects. A mysterious spot was found in SN1987A using the speckle technique (Meikle et al. 1987; Nisenson et al. 1987). Many models including the jet model were proposed (Rees 1987; Piran & Nakamura 1987). At that time, it was difficult to distinguish each model from observations since only one spot was found. In the jet model, the counter jet should be observed although it is dim due to the redshift (Piran & Nakamura 1987). However, later in 1999, two spots were confirmed using a new software to analyze the speckle data (Nisenson & Papaliolios 1999). Very recently the jet feature of the ejecta of SN1987A whose position angle is the same as the mysterious spot was confirmed by HST (Wang et al. 2002). As a result the jet model by Piran & Nakamura (1987) took the advantage. Furthermore the observation of the counter jet may enable us to measure the Lorentz factor of the jet, as in the AGN and the microquasar. Therefore the argument on the observational properties of the emission from the counter jet of GRBs is urgent.

Let us consider the emission from the counter jet. The observed frequency is obtained by $\nu_{obs} \sim \delta \nu'_0$ where $\delta \equiv 1/\gamma(1 - \beta \cos \theta_v)$ is the Doppler factor, γ is the Lorentz factor of the jet and θ_v is the viewing angle of the jet. We adopt the typical frequency measured in the jet-comoving frame as $\nu'_0 \sim 1$ keV so that the forward jet is observed as the GRB, i.e., $\nu_{obs} \sim 2\gamma \nu'_0 \sim 200$ keV for $\theta_v \sim 0$, where we assume $\gamma \sim 100$. Then, since $\theta_v \sim \pi$ for the counter jet, $\delta \sim 1/2\gamma$ and hence $\nu_{obs} \sim 5$ eV, which is in the UV band. When we vary the Lorentz factor γ , ν_{obs} may be in the optical band. This transient phenomenon, whose timescale is equal to that of the forward jet emission, should be observed about several tens of hours after the forward jet emission, since each jet radiates almost simultaneously at the radius of order $10^{14} - 10^{15}$ cm. We call this event the *delayed flash* (DF).

The attempt to detect the DF might be difficult since the afterglow of the forward jet might be brighter than the DF. The afterglow of the GRB, i.e., the afterglow of the on-axis forward jet is much brighter than the DF. However if the forward jet is observed with the

large viewing angle, there is a chance to observe the DF since the forward jet emission is also dim at the time of the DF.

Recently, we studied the emission from the off-axis jet (Yamazaki, Ioka, & Nakamura 2002; see also Nakamura 2000; Ioka & Nakamura 2001a). We proposed that if we observe the GRB with a large viewing angle, it looks like the X-ray flash (XRF), a new class of X-ray transients which has been recently recognized as a phenomenon related to the GRB (e.g., Heise et al. 2001; Kippen et al. 2002). If $\gamma\theta_v \sim 15$ and hence $\delta \sim 1$, the typical frequency is in the X-ray band $\nu_{obs} \sim 1$ keV. In addition, we can explain various observational characteristics of the XRF, such as the peak flux ratio and the fluence ratio between the γ -ray and the X-ray band, the X-ray photon index, the typical duration, and the event rate (Yamazaki, Ioka, & Nakamura 2002). We suggested that *the origin of the XRF is identical to that of the GRB*.

In this Letter, we will show that the DF can be observed after the XRF. We will calculate the light curve of the XRF, the DF, and the afterglow of the XRF, and discuss whether the DF can be detected by current instruments such as Far-Ultraviolet Multi-Anode Microchannel Array (FUV-MAMA) detector on *Hubble Space Telescope (HST)* Space Telescope Imaging Spectrograph (STIS), or future observational missions such as *Swift*. In § 2, we describe a simple forward- counter-jet model for the XRF and the DF. In § 3 and § 4, we show the light curves of the XRF, the DF, and the XRF afterglow. § 5 is devoted to a discussion.

2. MODEL DESCRIPTION

We extend the simple jet model by Yamazaki, Ioka & Nakamura (2002). We use a spherical coordinate system (r, θ, ϕ) in Lab frame, where the $\theta = 0$ axis points toward the detector, and the central engine is located at $r = 0$. The forward jet has a viewing angle, θ_v , which the axis of the emission cone makes with the $\theta = 0$ axis, while the counter jet has a viewing angle $\theta_v + \pi$. We adopt an instantaneous emission of infinitesimally thin shell at $t = t_0$ and $r = r_0$. Then the observed flux per unit frequency of a single pulse at the observed time T is given by

$$F_\nu(T) = \frac{2c^2\beta\gamma^4 A_0(r_0/c\beta\gamma^2) \Delta\phi(T)f[\nu\gamma(1 - \beta\cos\theta(T))]}{D^2 [\gamma^2(1 - \beta\cos\theta(T))]^2}, \quad (1)$$

where, $1 - \beta\cos\theta(T) = (c\beta/r_0)T$. A_0 determines the normalization of emissivity and $f(\nu')$ represents the spectral shape (For details, see Ioka & Nakamura 2001a; Granot, Piran & Sari 1999; Woods & Loeb 1999). A pulse-starting time and ending time are given as

$$T_{start}^{(XRF)} = (r_0/c\beta)(1 - \beta\cos(\max[0, \theta_v - \Delta\theta])), \quad (2)$$

$$T_{end}^{(XRF)} = (r_0/c\beta)(1 - \beta\cos(\theta_v + \Delta\theta)), \quad (3)$$

for the XRF, and

$$T_{start}^{(DF)} = (r_0/c\beta)(1 + \beta \cos(\theta_v + \Delta\theta)), \quad (4)$$

$$T_{end}^{(DF)} = (r_0/c\beta)(1 + \beta \cos(\max[0, \theta_v - \Delta\theta])), \quad (5)$$

for the DF. $\Delta\phi(T)$ is given as

$$\Delta\phi(T) = \begin{cases} \cos^{-1} \left[\frac{\cos \Delta\theta - \cos \theta(T) \cos \theta_v}{\sin \theta_v \sin \theta(T)} \right] & (\theta_v > \Delta\theta, \text{ or } \theta_v < \Delta\theta \text{ and } T_* < T < T_{end}^{(XRF)}) \\ \pi & (\theta_v < \Delta\theta \text{ and } T_{start}^{(XRF)} < T < T_*) \end{cases} \quad (6)$$

for the XRF where $T_* = (r_0/c\beta)\{1 - \beta \cos(\Delta\theta - \theta_v)\}$, and

$$\Delta\phi(T) = \begin{cases} \cos^{-1} \left[\frac{\cos \Delta\theta + \cos \theta(T) \cos \theta_v}{-\sin \theta_v \sin \theta(T)} \right] & (\theta_v > \Delta\theta, \text{ or } \theta_v < \Delta\theta \text{ and } T_{start}^{(DF)} < T < T_{**}) \\ \pi & (\theta_v < \Delta\theta \text{ and } T_{**} < T < T_{end}^{(DF)}) \end{cases} \quad (7)$$

for the DF where $T_{**} = (r_0/c\beta)\{1 + \beta \cos(\Delta\theta - \theta_v)\}$.

The spectrum of the GRB is well approximated by the Band spectrum (Band et al. 1993). In order to have a spectral shape similar to the Band spectrum, we adopt the following form of the spectrum in the comoving frame,

$$f(\nu') = (\nu'/\nu'_0)^{1+\alpha_B} (1 + \nu'/\nu'_0)^{\beta_B-\alpha_B}, \quad (8)$$

where α_B (β_B) is the low (high) energy power law index. In the GRB, $\alpha_B \sim -1$ and $\beta_B \sim -3$ are typical values (Preece et al. 2000). Equations (1) and (8) are the basic equations to calculate the flux of a single pulse, which depends on following parameters: $\gamma \gg 1$, $\theta_v \ll 1$, $\Delta\theta \ll 1$, $\gamma\nu'_0$, $\gamma\theta_v$, $\gamma\Delta\theta$, $r_0/c\beta\gamma^2$, α_B , β_B , D and A_0 .

Hereafter we will fix the following parameters: $\gamma = 100$, $\gamma\Delta\theta = 5$, $r_0/c\beta\gamma^2 = 1$ s, $\alpha_B = -1$, $\beta_B = -3$ and $\gamma\nu'_0 = 200$ keV. We fix the amplitude A_0 so that the isotropic γ -ray energy $E_{iso} = 4\pi D^2 S(20 - 2000 \text{ keV})$ equals 4×10^{53} erg when $\gamma\theta_v = 0$. Here $S(\nu_1 - \nu_2) = \int_{T_{start}}^{T_{end}} F(T; \nu_1 - \nu_2) dT$ is the observed fluence in the energy range $\nu_1 - \nu_2$ and $F(T; \nu_1 - \nu_2) = \int_{\nu_1}^{\nu_2} F_\nu(T) d\nu$ is the observed flux in the same energy range. Then, we obtain $A_0 = 7.3 \times 10^2 \text{ erg cm}^{-2} \text{ Hz}^{-1}$. Note that since $\gamma = 100$, the opening half-angle of the jet is similar to the observed one $\Delta\theta \sim 0.05$ and the total energy corrected for geometry is comparable to the observed value $(\Delta\theta)^2 E_{iso} \sim 10^{51}$ ergs (Frail et al. 2001).

We introduce dimensionless variables as $\tau = T/(r_0/c\beta\gamma^2)$ and $\xi = h\nu/\text{keV}$. Then, the observed flux can be rewritten as

$$F(\tau; \nu_{min} - \nu_{max}) = F_0 \tau^{\alpha_B-1} \Delta\phi(\tau) \int_{\xi_{min}}^{\xi_{max}} d\xi \xi^{1+\alpha_B} (1 + \xi\tau/\xi_0)^{\beta_B-\alpha_B}, \quad (9)$$

where, $\xi_0 = h\gamma\nu'_0/\text{keV}$ and $F_0 = 2cA_0r_0\gamma^3\nu'_0\xi_0^{-2-\alpha_B}/D^2$. For our parameters, we obtain¹

$$F_0 = 3.3 \times 10^{-6} \text{ ergs s}^{-1} \text{ cm}^{-2} D_{\text{Gpc}}^{-2} \left(\frac{A_0}{7.3 \times 10^2 \text{ ergs cm}^{-2} \text{ Hz}^{-1}} \right) \times \left(\frac{r_0/c\beta\gamma^2}{1 \text{ s}} \right) \left(\frac{\gamma}{100} \right)^4 \left(\frac{h\gamma\nu'_0}{200 \text{ keV}} \right)^{-1-\alpha_B}, \quad (10)$$

where $D_{\text{Gpc}} = D/\text{Gpc}$.

3. LIGHT CURVES OF X-RAY FLASH AND DELAYED FLASH

In this section, we draw the light curves of the XRF and the DF using Eq.(9), and discuss whether these events can be observed by current and future detectors.

At first, we show the light curves of the XRF $F(\tau; 2 - 25 \text{ keV})$ in Figure 1 with varying $\gamma\theta_v$. The observation band corresponds to that of the Wide-field X-ray Monitor (WXM) on HETE-2. As $\gamma\theta_v$ increases, the peak flux of the XRF $F_{\text{peak}}^{(\text{XRF})}$ decreases due to the relativistic beaming effect.

The light curves of the DF $F(\tau; 7.3 - 11 \text{ eV})$ are shown in Figure 2 with varying $\gamma\theta_v$. The observation band corresponds that of FUV-MAMA on *HST*/STIS. We find that the flux remains almost constant in each pulse, and that the peak flux $F_{\text{peak}}^{(\text{DF})}$ changes factor two or three when the viewing angle $\gamma\theta_v$ is varied. One can explain this behavior as follows. The value of $\theta(T)$ ranges between $\pi + \max\{0, \theta_v - \Delta\theta\}$ and $\pi + \theta_v + \Delta\theta$, which implies that the Doppler factor in each time $\delta = 1/\gamma(1 - \beta \cos \theta(T))$ is almost constant and nearly equals to $1/2\gamma$. Since we fix the spectral shape, $F_\nu(T)$ depends mainly on δ as $F_\nu \propto \delta^{1-\alpha_B} (\delta^{1-\beta_B})$ in the case of $\nu < \delta\nu'_0$ ($\nu > \delta\nu'_0$). Therefore, the flux of the delayed flash is almost constant with both the observed time and the viewing angle.

The peak flux of the DF can be estimated as follows. In the integrand of Eq. (9), ξ is an order of 10^{-3} since $\xi_{\text{max}} \sim \xi_{\text{min}} \sim 10^{-3}$, which implies that the integrand of Eq. (9) is an order of unity (mean value is about 0.3 for our parameters). The maximum value of $\Delta\phi$ is about $\Delta\theta/\theta_v$. Therefore, one can see $F_{\text{peak}}^{(\text{DF})}/F_0 \sim (2\gamma^2)^{\alpha_B-1} (\Delta\theta/\theta_v) \cdot 0.3 \cdot (\xi_{\text{max}} - \xi_{\text{min}}) \sim 10^{-12}(\gamma\theta_v/15)^{-1}$.

¹When we consider the effect of cosmology ($\Omega_M = 0.3$, $\Omega_\Lambda = 0.7$, and $h = 0.7$), $D \sim 1 \text{ Gpc}$ corresponds to $z \sim 0.2$. Since we consider the case $D < 1 \text{ Gpc}$ in the following sections, this does not affect our argument qualitatively but alters the quantitative results up to a factor of 2.

3.1. Detectability with Current Instruments

At present, FUV-MAMA on *HST*/STIS has been in operation, which has an observation band 7.3-11 eV. The field of view of FUV-MAMA is so small that the position of the event should be determined by localizing the preceding XRF with WXM on HETE-2, which have observation bands 2-25 keV. The limiting sensitivity of FUV-MAMA (WXM) is about $3 \times 10^{-14} \text{ ergs s}^{-1} \text{ cm}^{-2}$ ($10^{-9} \text{ ergs s}^{-1} \text{ cm}^{-2}$) for an event with a duration of $\sim 10^2$ seconds. One can see that the DF can be detected when the distance to the source D is smaller than 0.01 Gpc. Then, if $\gamma\theta_v \lesssim 36$, WXM can detect the preceding XRF.

3.2. Detectability with Instruments on *Swift*

The *Swift* satellite carries the Burst Alert Telescope (BAT) and Ultraviolet and Optical Telescope (UVOT), which have observation bands 15-150 keV and 1.9-7.3 eV, respectively. The limiting sensitivity of the BAT (UVOT) can be estimated as $10^{-10} \text{ ergs s}^{-1} \text{ cm}^{-2}$ ($5 \times 10^{-15} \text{ ergs s}^{-1} \text{ cm}^{-2}$) for a duration of $\sim 10^2$ seconds. The BAT localizes the XRF and the following observation by the UVOT may identify the associated DF. One can see that the DF with $D \lesssim 0.03$ Gpc is observable. Then the BAT can detect the preceding XRF if $\gamma\theta_v \lesssim 30$.

4. AFTERGLOW OF X-RAY FLASH

The start and the end time of the DF is about $T_{start}^{(DF)} \sim T_{end}^{(DF)} \sim 2\gamma^2(r_0/c\beta\gamma^2) \sim 2 \times 10^4 \text{ sec}$ for $\gamma = 10^2$ and $r_0/c\beta\gamma^2 = 1 \text{ sec}$. Therefore, one should compare the flux of the DF with that of the XRF afterglow. In this section, we draw the light curves of the XRF afterglow and see whether the DF can be detected or not. We use the simple model of the off-axis afterglow emission from the collimated jet (Model 1 of Granot et al. 2002).

For $\theta_v = 0$, the standard afterglow model, i.e., the synchrotron-shock model, can explain observational properties of the GRB afterglow very well (Piran, 1999), and gives the observed flux per unit frequency as $F_\nu(T; \theta_v = 0) = F_\nu^{(R-SPH)} \equiv G(\nu, T)$, where $F_\nu^{(R-SPH)}$ is the observed flux given by Rhoads (1999) and Sari, Piran & Halpern (1999). For $\theta_v > \Delta\theta$, the emission is assumed to be from a point source moving along the jet axis. Then the flux is given by $F_\nu(T; \theta_v) = a^3 G(a^{-1}\nu, aT)$, where $a \equiv (1 - \beta)/(1 - \beta \cos \tilde{\theta}) \sim (1 + (\gamma\tilde{\theta})^2)^{-1}$. We choose $\tilde{\theta} = \max(0, \theta_v - \Delta\theta)$ to make this simple model more realistic (Granot et al. 2002).

The Lorentz factor of the shell γ can be determined by

$$\gamma\Delta\theta = \begin{cases} (aT/t_{jet})^{-3/8} & \text{if } aT < t_{jet} \\ (aT/t_{jet})^{-1/2} & \text{if } aT > t_{jet}, \end{cases} \quad (11)$$

where $t_{jet} = 2.1 \times 10^4 \text{sec} n^{-1/3} (\Delta\theta/0.1)^{8/3} (E/10^{52} \text{ergs})^{1/3}$ is the jet-break time observed from an on-axis observer ².

Using above equations, we calculate the light curves of the afterglow. In order to study the dependence on the viewing angle θ_v , we fix the rest of the parameters: the power-law index of accelerated electrons $p = 2.25$, the number density of the ambient matter $n = 1 \text{cm}^{-3}$, total energy of the shock $E = 2 \times 10^{54} \text{ergs}$, $\varepsilon_e = 0.1$ and $\varepsilon_B = 0.01$, and the distance $D = 30 \text{Mpc}$. We show the results in Figure 3. The observation band is 1.9-7.3 eV, which corresponds that of UVOT.

We also plot the UV flux of the DF in the same figure. Since the duration of the DF $\sim 10^2 \text{sec}$ is short, the light curve of the DF is plotted as a point and degenerated. We can see that the UV flux of the DF dominates the afterglow when $\theta_v \gtrsim 0.18$. If we alter the observation band to 7.3-11 eV, this threshold value remains unchanged.

5. DISCUSSION

We have calculated the light curves of the DF, the XRF, and the afterglow of the XRF, and shown that the DF could be observed in the UV band about $10^4 - 10^5$ seconds after the XRF by current or future detectors such as FUV-MAMA on *HST*/STIS or UVOT on *Swift*. Note that since the UV flux of the GRB afterglow is much larger than that of the DF, only the DF associated with the XRF has a chance to be observed. Following Yamazaki, Ioka, & Nakamura (2002), we can roughly estimate the event rate of the DF with the instruments on *Swift* as

$$R_{DF} \sim 1 \times 10^{-3} \text{events yr}^{-1} \left(\frac{r_{GRB}}{5 \times 10^{-8} \text{events yr}^{-1} \text{galaxy}^{-1}} \right) \left(\frac{D_{DF}}{0.03 \text{Gpc}} \right)^3 \\ \times \left(\frac{n_g}{10^{-2} \text{galaxies Mpc}^{-3}} \right) \left(\frac{f_{DF}/f_{GRB}}{23} \right), \quad (12)$$

where r_{GRB} and n_g are the event rate of the GRBs and the number density of galaxies, respectively. f_{DF} (f_{GRB}) is the solid angle subtended by the direction to which the source is

²For simplicity, we assume the relation $t' = R/(4\gamma^2 c)$, where t' and R are the time measured by an on-axis observer and the radius of the shock.

observed as the DF (GRB), and $f_{DF}/f_{GRB} = (0.3^2 - 0.18^2)/0.05^2 = 23$. This value is small, however, if the distance is similar to GRB980425, we will detect the DF. A similar estimate for the current detectors gives smaller value $\sim 10^{-4}$ events yr^{-1} .

We need the next-generation detectors, which are more sensitive than the instruments on *Swift*, to detect the DF associated with very dim XRF more frequently. For example, if the UV band detector has an observation band 0.2-20 eV and a sensitivity of $10^{-17} \text{ ergs s}^{-1} \text{ cm}^{-2}$, we can observe the DF with the distance of $D \sim 1 \text{ Gpc}$. And suppose the X-ray band burst monitor has an observation band 2-25 keV and a sensitivity of $2 \times 10^{-14} \text{ ergs s}^{-1} \text{ cm}^{-2}$, Then, we can observe the preceding XRF with $\gamma\theta_v \lesssim 40$, which occurs at $D \sim 1 \text{ Gpc}$. The event rate can be estimated as $\sim 10^2$ events yr^{-1} .

The DF may be obscured by the dust extinction. In fact, about half of accurately localized GRBs do not produce a detectable optical afterglow (Fynbo et al. 2001; Lazzati, Covino & Ghisellini 2002). One explanation for these “dark GRBs” is that most GRBs occur in giant molecular clouds (e.g., Reichart & Price 2002). In this picture, a GRB has a detectable optical afterglow only if the burst and the afterglow destroy the dust along the line of sight to the observer (Waxman & Draine 2000; Fruchter, Krolik & Rhoads 2001), as suggested by the comparison between the X-ray and optical extinction (Galama & Wijers 2001). In this case the DF is obscured since the flux of the XRF is too dim to carve out a path for the DF. However this picture may have some problems, such as no evidence of an ionized absorber (Piro et al. 2002) and the variable column density in the X-ray afterglow (Djorgovski et al. 2001c). There are other explanations for the dark GRBs, such as the high redshift effects, the dust extinction in the inter stellar medium of the host galaxy (Ramirez-Ruiz, Trentham & Blain 2002; Piro et al. 2002) and so on. Therefore at present we cannot conclude that the DF is obscured.

If we assume that the absolute magnitude of the host galaxy is about $\sim -20 \text{ mag}$ (Djorgovski et al. 2001a, b), the apparent magnitude is about $\sim 15 + 5 \log D_{\text{Gpc}}$. Since the host galaxy with the size $\sim 10 \text{ kpc}$ has an angular size of $\sim 10 D_{\text{Gpc}}^{-1} \text{ arcsec}$, we can observe a point source which is dimmer than the host galaxy by $\sim 10^{-4} D_{\text{Gpc}}^2$ if the angular resolution is $\sim 0.1 \text{ arcsec}$. Therefore the DF has to be brighter than $\sim 25 \text{ mag}$, and hence we can observe the DF if $D \lesssim 0.03 \text{ Gpc}$.

If the GRB is associated with the supernova (SN), the emission from the SN may hide the DF. The UV flux of SN1998bw was about $\sim 17 \text{ mag}$ at the distance $D \sim 0.04 \text{ Gpc}$ (Galama et al. 1998), i.e., $\sim 6 \times 10^{-15} D_{\text{Gpc}}^{-2} \text{ erg s}^{-1} \text{ cm}^{-2}$, so that the SN like SN1998bw is brighter than the DF. However at present it is not clear whether all GRBs are associated with the SNe or not (e.g., Price et al. 2002). In any cases, deep searches following the XRF will give us valuable information.

If the DF associated with the XRF is observed, we will be able to estimate or determine the Lorentz factor and the viewing angle of the jets. Let the typical frequency or the break energy of the DF (XRF) be $\nu_{DF} = \delta_{DF}\nu'_0$ ($\nu_{XRF} = \delta_{XRF}\nu'_0$). When $\theta_v \ll 1$, $\gamma \gg 1$ and $(\gamma\theta_v)^2 \gg 1$, we can derive $\delta_{DF} \sim 1/(2\gamma)$ and $\delta_{XRF} \sim 2\gamma/(\gamma\theta_v)^2$. Since we assume that the XRF is the GRB observed from off-axis viewing angle, we can use the observational consequence for the break energy $\delta_{GRB}\nu'_0 \sim 200$ keV, where $\delta_{GRB} \sim 2\gamma$ (Preece et al. 2000). Then, we obtain $\nu_{DF}/200 \text{ keV} \sim (2\gamma)^{-2}$. Therefore, ν_{DF} will tell us the Lorentz factor of the jet. On the other hand, we can derive $\nu_{DF}/\nu_{XRF} \sim (\theta_v/2)^2$, which implies that we can determine the viewing angle.

There is also the emission from the reverse shock of the counter jet. The reverse shock emission for $\theta_v = 0$ peaks at $T_0 \sim 10$ s for the thin shell case (Kobayashi 2000; Sari & Piran 1999a, b). At the peak time, the synchrotron typical frequency and the peak flux is about $\nu_m \sim 10^{14}$ Hz and $F_{\nu, max} \sim 10D_{Gpc}^{-2}$ Jy, respectively. For the counter jet, the viewing angle is about π and $a \sim 1/4\gamma^2 \sim 10^{-4}$. Thus the typical synchrotron frequency is about $\nu_m \sim 10^{10}a_{-4}$ Hz, which is in the radio band. The emission occurs at about $T \sim 10^5a_{-4}^{-1}$ s. The peak flux at ν_m is about $F_{\nu, max} \sim 10^{-11}a_{-4}^3D_{Gpc}^{-2}$ Jy. This may be too dim to be observed with the current detectors.

We are grateful to A. Yoshida and T. Murakami for helpful comments. This work was supported in part by Grant-in-Aid for Scientific Research of the Japanese Ministry of Education, Culture, Sports, Science and Technology, No.00660 (KI), No.14047212 (TN), and No.14204024 (TN).

REFERENCES

- Band, D., et al. 1993, ApJ, 413, 281
- Begelman, M. C., Blandford, R. D., & Rees, M. J. 1984, Rev. Mod. Phys., 56, 255
- Dado, S., Dar, A., & De Rújula, A., 2001, astro-ph/0107367
- Djorgovski, S. G., et al. 2001a, astro-ph/0106574
- Djorgovski, S. G., et al. 2001b, astro-ph/0107535
- Djorgovski, S. G., et al. 2001c, ApJ, 562, 654
- Frail, D., A., et al. 2001, ApJ, 562, L55

- Fruchter, A., Krolik, J. H., & Rhoads, J. E. 2001, *ApJ*, 563, 597
- Fynbo, J. U., et al. 2001, *A&A*, 369, 373
- Galama, T. J., et al. 1998, *Nature*, 395, 670
- Galama, T. J., & Wijers, R. A. M. 2001, *ApJ*, 549, L209
- Ghisellini, G., & Lazzati, D. 1999, *MNRAS*, 309, L7
- Granot, J., Panaitescu, A., Kumar, P., & Woosley, S. E. 2002, *ApJ*, 570, L61
- Granot, J., Piran, T., & Sari, R. 1999, *ApJ*, 513, 679
- Heise, J., in 't Zand, J., Kippen, R. M., & Woods, P. M. 2001, in *Proc. Second Rome Workshop: Gamma-Ray Bursts in the Afterglow Era* (Berlin: Springer), astro-ph/0111246
- Huang, Y. F., Dai, Z. G., & Lu, T. 2002, *MNRAS* in press
- Ioka, K., & Nakamura, T. 2001a, *ApJ*, 554, L163
- Ioka, K., & Nakamura, T. 2001b, *ApJ*, 561, 703
- Kippen, R. M., et al. 2002, in *Proc. Woods Hole Gamma-Ray Burst Workshop*, astro-ph/0203114
- Kobayashi, S. 2000, *ApJ*, 545, 807
- Lazzati, D., Covino, S., & Ghisellini, G. 2002, *MNRAS*, 330, 583
- Meikle, W. P. S., et al. 1987, *Nature*, 329, 608
- Mirabel, I. F., & Rodríguez, L. F. 1999, *ARA&A*, 37, 409
- Nakamura, T. 2000, *ApJ*, 534, L159
- Nisenson, P., et al. 1987, *ApJ*, 320, L15
- Nisenson, P. & Papaliolios, C., 1999, *ApJ*, 518, L29
- Piran, T. 1999, *Phys. Rep.*, 314, 575
- Piran, T. & Nakamura, T., 1987, *Nature*, 330, 28
- Piro, L., et al. 2002, astro-ph/0201282

- Preece, R. D., Briggs, M. S., Mallozzi, R. S., Pendleton, G. N., Paciesas, W. S., & Band, D. L. 2000, *ApJS*, 126, 19
- Price, P. A., et al. 2002, *astro-ph/0207187*
- Ramirez-Ruiz, E., Trentham, N., & Blain, A. W. 2002, *MNRAS*, 329, 465
- Reichart, D. E., & Price, P. 2002, *ApJ*, 565, 174
- Rees, M. J., 1987, *Nature*, 328, 207
- Rhoads, J. E., 1999, *ApJ*, 525, 737
- Sari, R. 1999, *ApJ*, 524, L43
- Sari, R., & Piran, T. 1999a, *ApJ*, 520, 641
- Sari, R., & Piran, T. 1999b, *ApJ*, 517, L109
- Sari, R., Piran, T., & Halpern, J. P. 1999, *ApJ*, 519, L17
- Totani, T., & Panaitescu, A. 2002, *astro-ph/0204258*
- Wang, L., et al., *astro-ph/0205337*
- Waxman, E., & Draine, B. T. 2000, *ApJ*, 537, 796
- Woods, E., & Loeb, A. 1999, *ApJ*, 523, 187
- Yamazaki, R., Ioka, K., & Nakamura, T. 2002, *ApJ*, 571, L31

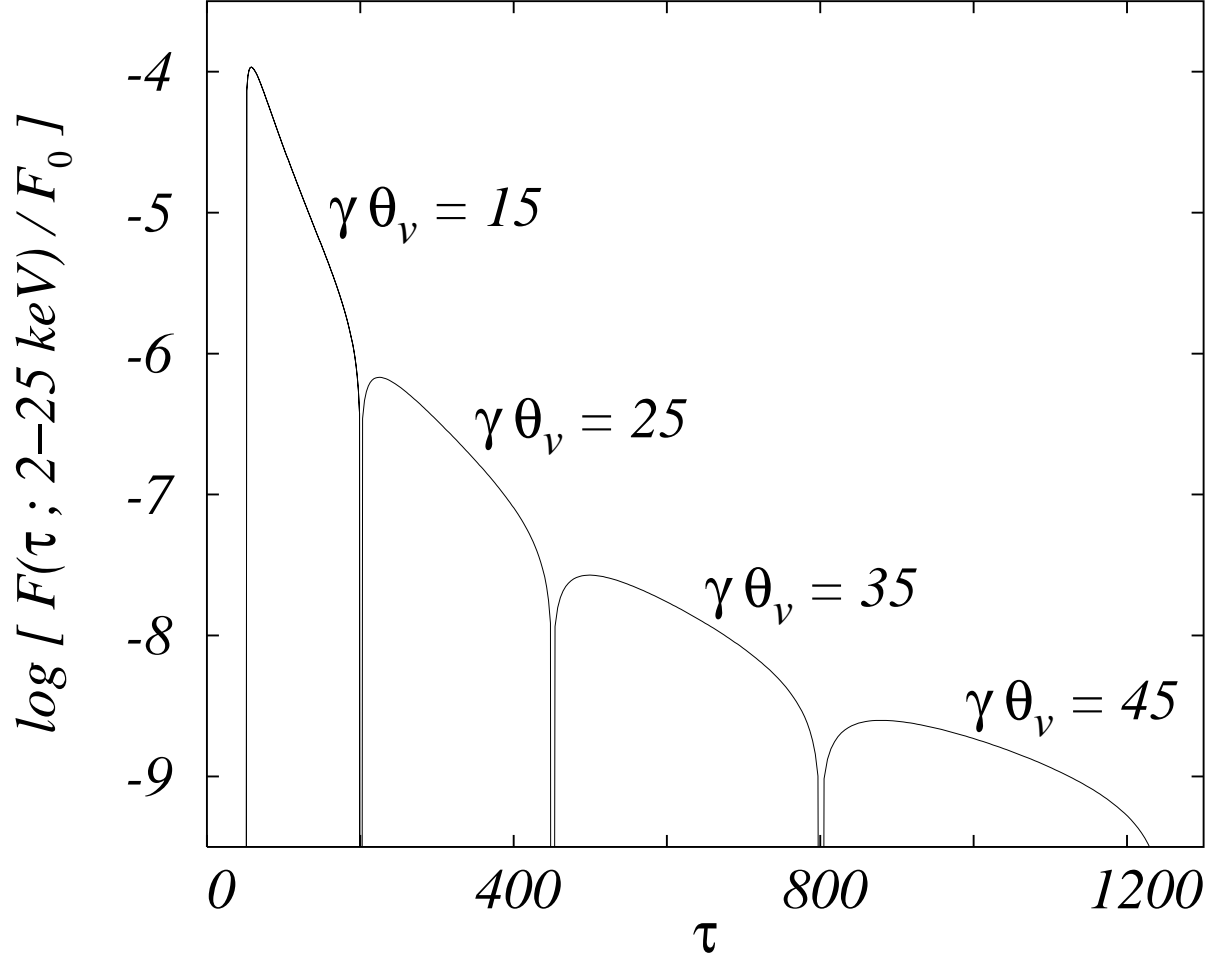


Fig. 1.— The light curve of the X-ray flash as a function of the normalized observed time $\tau = T/(r_0/c\beta\gamma^2)$, where we adopt $r_0/\beta c\gamma^2 = 1$ sec. We choose $\gamma\Delta\theta = 5$, $\alpha_B = -1$, $\beta_B = -3$, and $\gamma\nu'_0 = 200$ keV. The flux-normalization constant is $F_0 = 3.3 \times 10^{-6} D_{\text{Gpc}}^{-2} \text{ ergs s}^{-1} \text{ cm}^{-2}$.

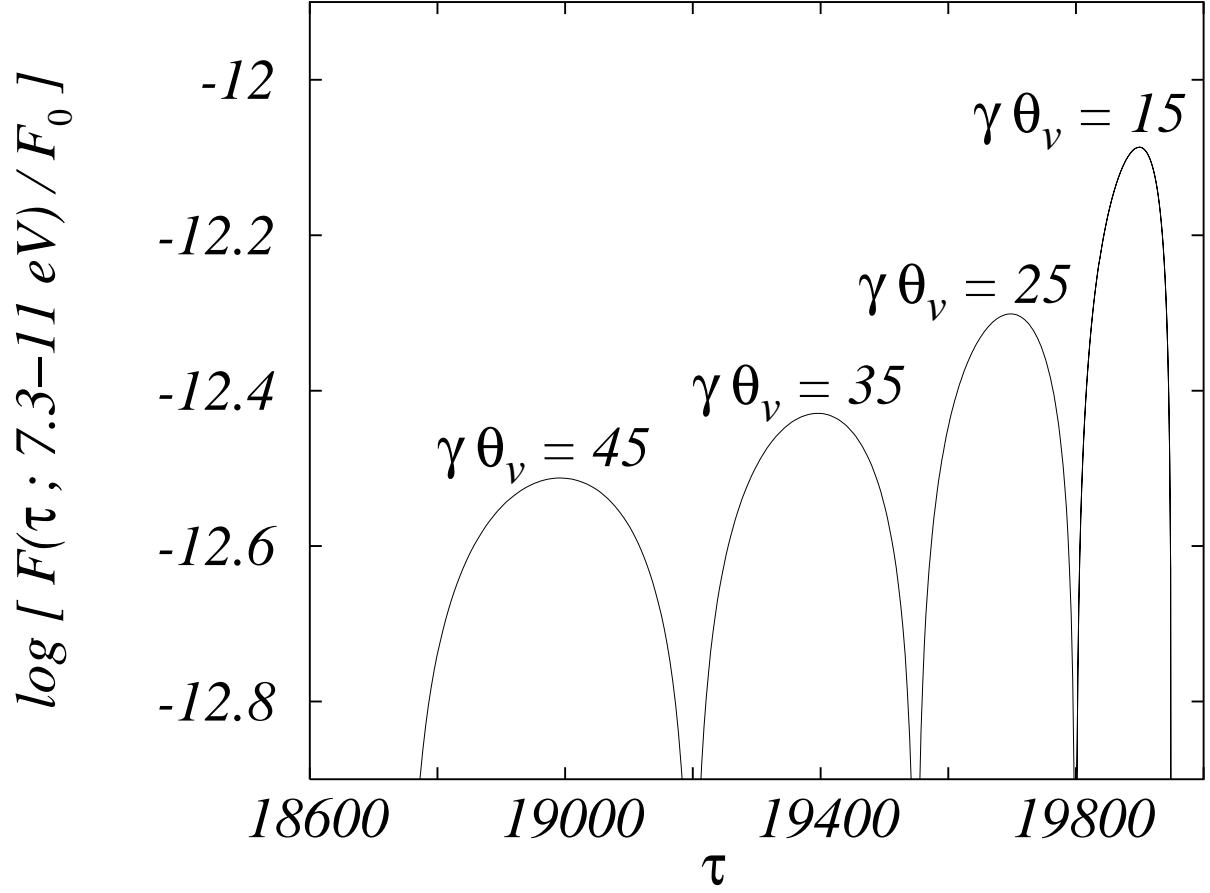


Fig. 2.— The light curve of the *delayed flash* as a function of the normalized observed time $\tau = T/(r_0/c\beta\gamma^2)$, where we adopt $r_0/\beta c\gamma^2 = 1$ sec. We choose $\gamma = 100$, $\gamma\Delta\theta = 5$, $\alpha_B = -1$, $\beta_B = -3$, and $\gamma\nu'_0 = 200$ keV. The flux-normalization constant is $F_0 = 3.3 \times 10^{-6} D_{\text{Gpc}}^{-2} \text{ ergs s}^{-1} \text{ cm}^{-2}$. Our jet model predicts that compared with the light curve of the X-ray flash, the flux of the delayed flash is almost constant ($F \sim 3 \times 10^{-18} D_{\text{Gpc}}^{-2} \text{ ergs s}^{-1} \text{ cm}^{-2}$) with both the observed time and the viewing angle.

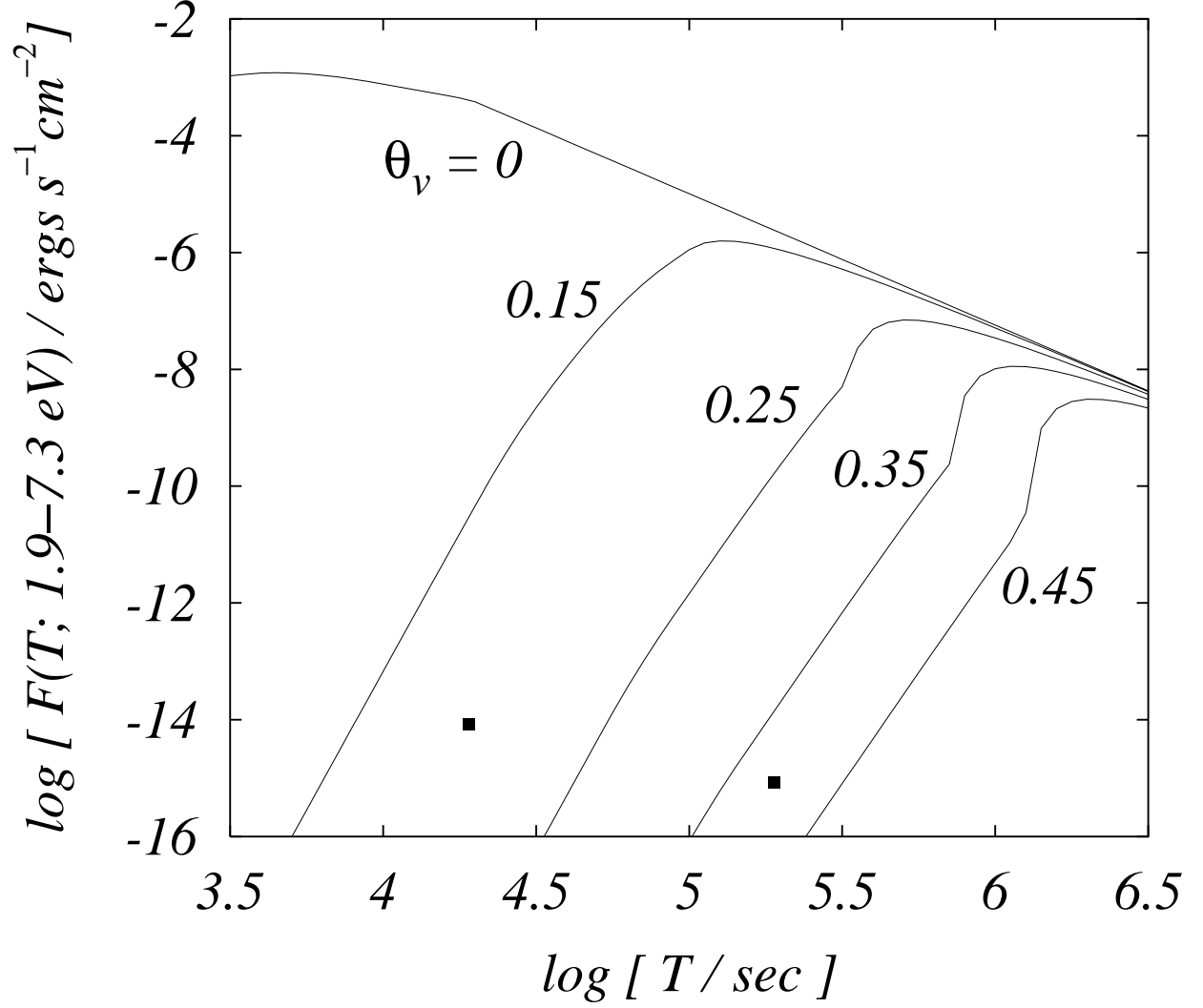


Fig. 3.— The light curves of the X-ray flash afterglow in the UV band are shown by varying the viewing angle θ_v . We fix parameters as $n = 1 \text{ cm}^{-3}$, $p = 2.25$, $E = 2 \times 10^{54} \text{ ergs}$, $\Delta\theta = 0.05$, $\varepsilon_e = 0.1$, $\varepsilon_B = 0.01$, and $D = 30 \text{ Mpc}$. Two filled squares represent the UV flux of the *delayed flash*. The left one corresponds to the case $r_0/\beta c\gamma^2 = 1 \text{ sec}$, while the right one $r_0/\beta c\gamma^2 = 10 \text{ sec}$.